Role of ammonia-oxidizing microorganisms in the removal of organic micropollutants during simulated riverbank filtration

Zhao, Jian; Fang, Shangbiao; Liu, Gang; Qi, Weixiao; Bai, Yaohui; Liu, Huijuan; Qu, Jiuhui

DOI
10.1016/j.watres.2022.119250

Publication date
2022

Document Version
Final published version

Published in
Water Research

Water Research 226 (2022) 119250

Contents lists available at ScienceDirect

Water Research

journal homepage: www.elsevier.com/locate/watres

Role of ammonia-oxidizing microorganisms in the removal of organic micropollutants during simulated riverbank filtration

Jian Zhao [a], Shangbiao Fang [a], Gang Liu [b,c], Weixiao Qi [a,d], Yaohui Bai [b], Huijuan Liu [a,d,*], Jiuhui Qu [a]

[a] Center for Water and Ecology, State Key Joint Laboratory of Environment Simulation and Pollution Control, School of Environment, Tsinghua University, Beijing 100084, China
[b] Key Laboratory of Drinking Water Science and Technology, Research Centre for Eco-Environmental Sciences, Chinese Academy of Sciences, Beijing 100085, China
[c] Sanitary Engineering, Department of Water Management, Faculty of Civil Engineering and Geosciences, Delft University of Technology, P.O. Box 5048, 2600GA, Delft, the Netherlands
[d] Beijing Laboratory of Environmental Frontier Technologies, School of Environment, Tsinghua University, Beijing 100084, China

ARTICLE INFO

Keywords:
Riverbank filtration
Organic micropollutants
First-meter infiltration
Biodegradation
Ammonia-oxidizing microorganisms

ABSTRACT

Biodegradation plays an important role in the removal of organic micropollutants (OMPs) during riverbank filtration (RBF) for drinking water production. The ability of ammonia-oxidizing microorganisms (AOM) to remove OMPs has attracted increasing attention. However, the distribution of AOM in RBF and its role in the degradation of OMPs remains unknown. In this study, the behavior of 128 selected OMPs and the distribution of AOM and their roles in the degradation of OMPs in RBF were explored by column and batch experiments simulating the first meter of the riverbank. The results showed that the selected OMPs were effectively removed (82/128 OMPs, >70% removal) primarily by biodegradation and partly by adsorption. Inefficiently removed OMPs tended to have low molecular weights, low log P, and contain secondary amides, secondary sulfonamides, secondary ketimines, and benzyls. In terms of the microbial communities, the relative abundance of AOM increased from 0.1%–0.2% ($inlet_{sand}$) to 5.3%–5.9% ($outlet_{sand}$), which was dominated by ammonia-oxidizing archaea whose relative abundance increased from 23%–72% ($inlet_{sand}$) to 97% ($outlet_{sand}$). Comammox accounted for 23%–64% in the $inlet_{sand}$ and 1% in the $outlet_{sand}$. The abundances of AOM *amo*A genes kept stable in the $inlet_{sand}$ of control columns, while decreased by 78% in the treatment columns, suggesting the inhibition effect of allylthiourea (ATU) on AOM. It is observed that AOM played an important role in the degradation of OMPs, where its inhibition led to the corresponding inhibition of 32 OMPs (5/32 were completely suppressed). In particular, OMPs with low molecular weights and containing primary amides, secondary amides, benzyls, and secondary sulfonamides were more likely to be removed by AOM. This study reveals the vital role of AOM in the removal of OMPs, deepens our understanding of the degradation of OMPs in RBF, and offers valuable insights into the physiochemical properties of OMPs and their AOM co-metabolic potential.

1. Introduction

Worldwide, organic micropollutants (OMPs, e.g., pharmaceutical and personal care products, pesticides, hormones) are continuously discharged into rivers, mainly as effluents from wastewater treatment plants and non-point sources, thereby causing increasing ecological risks (Kondor et al., 2020; Li et al., 2021; Loos et al., 2013; Miyawaki et al., 2021). These have been commonly detected and reported in drinking water sources. A study in Switzerland detected 75–96 out of the 461 targeted OMPs in the surface and ground water of RBF sites along the rivers Birs, Ergolz and Frenke, while 52 out of the 111 selected OMPs were detected in the Danube in Hungary (52 were detected in the Danube, and 32 were present in drinking water wells), and 36 out of the targeted 194 OMPs were observed in two sites at the Ems River and two at the Ruhr River in Germany (Oberleitner et al., 2020; Kondor et al., 2020; Hollender et al., 2018). The concentrations of OMPs detected in the water sources range from a few to several hundred ng/L, thereby posing a severe threat to public drinking water safety (Borrull et al.,

* Corresponding author at: Center for Water and Ecology, State Key Joint Laboratory of Environment Simulation and Pollution Control, School of Environment, Tsinghua University, Beijing 100084, China.
E-mail address: hjliu@tsinghua.edu.cn (H. Liu).

https://doi.org/10.1016/j.watres.2022.119250
Received 23 May 2022; Received in revised form 8 October 2022; Accepted 13 October 2022
Available online 14 October 2022

2021).

Riverbank filtration (RBF) is used globally as a drinking water pretreatment technology and has been widely reported as an effective barrier to OMPs (Hamann et al., 2016; Hollender et al., 2018; Zhai et al., 2022). The dissolved oxygen (DO) in the river water is gradually consumed during the infiltration process, forming unique aerobic, suboxic, and anoxic zones (Bertelkamp et al., 2016; Bai et al., 2019). The aerobic zone, commonly referred to as the first meter of infiltration, is the most active biochemical reaction zone, where the greatest attenuation of OMPs is observed (Hollender et al., 2018). OMPs can be removed via various mechanisms, including microbial biodegradation, adsorption, phytodegradation, hydrolysis, and volatilization in RBF, of which microbial biodegradation is generally recognized as the most important mechanism (Hamann et al., 2016; Bertelkamp et al., 2014; Zhao et al., 2022).

Ammonia-oxidizing microorganisms (AOM) include ammonia-oxidizing bacteria (AOB), ammonia-oxidizing archaea (AOA) and comammox. The presence of AOB and AOA in RBF has been reported (Junier et al., 2010; Zuo et al., 2021), but not comammox yet. Based on the reports of comammox's presences in both aquifer and drinking water system (Fowler et al., 2018; Wang et al., 2017), it is reasonable to speculate that comammox would be present in RBF. It is generally accepted that AOA and comammox are dominant over AOB under low NH_4^+ and oligotrophic conditions (Kits et al., 2017). Hence, we hypothesize that the AOM in RBF system would be dominated by comammox and AOA. It has been widely reported that AOM are closely related to OMPs degradation in wastewater treatment plants (WWTP) or in pure culture studies (Xu et al., 2017; Kassotaki et al., 2016; Rattier et al., 2014; Su et al., 2021; Zhou et al., 2021). AOA biotransformed mianserin and ranitidine with 3–5 times higher efficiency than AOB (Men et al., 2016); lincomycin could be degraded by AOA (hydroxylation, S-oxidation, and demethylation) and comammox (hydroxylation, demethylation, and demethylthioation), but not by AOB (Zhou et al., 2021). These findings suggests that the ability, efficiency, and reaction type during OMPs degradation of AOA, AOB and comammox could be different. The variations may be attributed to their different ammonia affinities (e.g., AOA > AOB, comammox > many AOA and AOB), ammonia conversion pathway (i.e., AOB and AOA oxide ammonia to nitrite, while comammox oxides ammonia to nitrate) and enzymatic repertoires (e.g., AOB and comammox induce hydroxylamine oxidoreductase, but AOA may not; only comammox generate nitrite oxidoreductase) (Zhou et al., 2019; Stein, 2019; Men et al., 2016; Kits et al., 2017; Zhou et al., 2021). Since AOM niche can be affected by NH_4^+ concentration, the observed OMPs degradations by AOM in high NH_4^+concentration WWTP may be not applicable in low NH_4^+ concentration RBF systems (Limpiyakorn et al., 2011; Covatti and Grischek, 2021). To better understand, manage and enhance OMPs degradation in RBF system, it is highly necessary to explore the AOM niche and their role in OMPs degradation.

In this study, 128 OMPs with a high detection frequency in surface water were selected as targets. The removal of these selected OMPs was studied via batch tests and a series of one-meter sand columns simulating the first-meter infiltration of the RBF. The abundances of bacteria, archaea, and AOM were measured using quantitative polymerase chain reaction (qPCR). The role of AOM in the degradation of OMPs was explored by running the columns with and without inhibiting AOM with ATU. The correlations between the inhibition ratio and physiochemical properties of OMPs, including log P, molecular weight (MW), and the type and quantity of nitrogen-containing functional groups, were determined based on the data set.

2. Materials and methods

2.1. Chemicals

A total of 128 OMPs were selected based on the prescription frequency, sales data, environmental priority, or medical use (Zhang et al., 2020; Bu et al., 2013; Robles-Molina et al., 2014). Their concerns and detailed information are listed in Table S1 of the Supporting Information. The OMPs with a purity of 95% or higher as powders or 100 $\mu g \cdot mL^{-1}$ as solution were procured from Sigma-Aldrich (USA) or First Standard (China) and stored at −20°C. Twenty-eight internal standards were procured from First Standard (China) as 100 $\mu g \cdot mL^{-1}$ solutions and stored at −20 °C (Table S2). Methanol (99.9%, Fisher, USA) and acetonitrile (99.9%, Fisher) were used as the solvent and mobile phase for liquid chromatography, respectively. ATU (98%) and formic acid (99.9%) were procured from Aladdin (China); ATU was used as an inhibitor to AOM. The solid-phase extraction (SPE) cartridges, Oasis HLB (500 mg, 6 mL), were procured from Waters (USA).

2.2. Column experiments

The experimental setup (Fig. 1) consisted of four black PVC columns ($L = 1$ m, $D = 36$ mm) filled with natural river sand ($d = 0.7$–2 mm, $d_{50} = 1$ mm). The two columns are duplicate control groups, abbreviated as C $_{ctrl-1}$ and C $_{ctrl-2}$, and the remaining two columns are duplicate treatment groups, abbreviated as C $_{tret-1}$ and C $_{tret-2}$. Sand parameters, namely grain size distribution, soil organic matter content (SOM), pH—H_2O, and cation exchange capacity (CEC), were analyzed. The results are presented in Table S3. The water supply for the columns was collected from the Yongding River (39°5958″ N, 116°447″ E, Beijing, China) and was updated weekly. The weekly analyzed water parameters (including DO, Ca, K, Mg, dissolved organic carbon [DOC], UV254, NH_4^+, F^-, Cl^-, SO_4^{2-}, and NO_3^-) are presented in Table S4. The columns were operated from bottom to top at room temperature (20°C–25°C), and the flow rate was approximately 0.25 L/d, which corresponded to the 36-h residence time estimated using the KBr tracer experiment. After a 6-month microbial cultivation period, 5 g of sand from the bottom (inlet$_{-sand)}$ and top (outlet$_{-sand}$) of each column were collected and stored at −80 °C for DNA extraction.

An 82-day OMP exposure experiment was subsequently conducted. The feed water was refreshed weekly, and 128 OMPs (100 ng/L of each) were added. The feed water was then filtered through 0.45-μm glass fiber filters before weekly refreshing to avoid the attenuation of OMPs in inlet flasks. Two control columns (C $_{ctrl-1}$ and C $_{ctrl-2)}$ were used to determine the removal efficiency of the OMPs. The continuous addition of 5 mg/L of ATU (inhibitor of AOM) to the feed water of the two treatment columns C $_{tret-1}$ and C $_{tret-2}$ was used to explore the effect of inhibiting AOM on the removal of OMPs. The concentrations of the influent OMPs were determined by measuring at three-time points in the first week ($T = 1$, 4, and 7 days) and then randomly six times in the following 75 days. The concentrations of the effluent OMPs were measured at 23 different time points over three months ($T = 1$, 2, 3, …,14, 21, 28, 35, 42, 49, 56, 63, 70, and 82 days).

2.3. Batch experiments

To estimate the contribution of sand adsorption to the removal of OMPs, a triple parallel batch test was performed. Control tests were assembled in brown flasks with 800 mL ultrapure water, 128 OMPs (100 ng/L each), and 400 mg/L NaN_3 to inhibit microbial activity. Treatment tests were assembled with 800 mL of water from the Yongding River, 200 g of natural river sand same as the column study, 128 OMPs (100 ng/L of each one), and 400 mg/L NaN_3. The flasks were incubated in a shaker incubator (25 °C, 120 rpm) for 36 h. The OMPs removed by adsorption were estimated by subtracting the residual concentration in the treatment tests from that in the control tests.

2.4. Analytical methods for OMPs

Water samples were pre-processed from 200 mL to 0.5 mL via SPE (Waters Oasis HLB, 6 cc/500 mg). The water sample was passed through

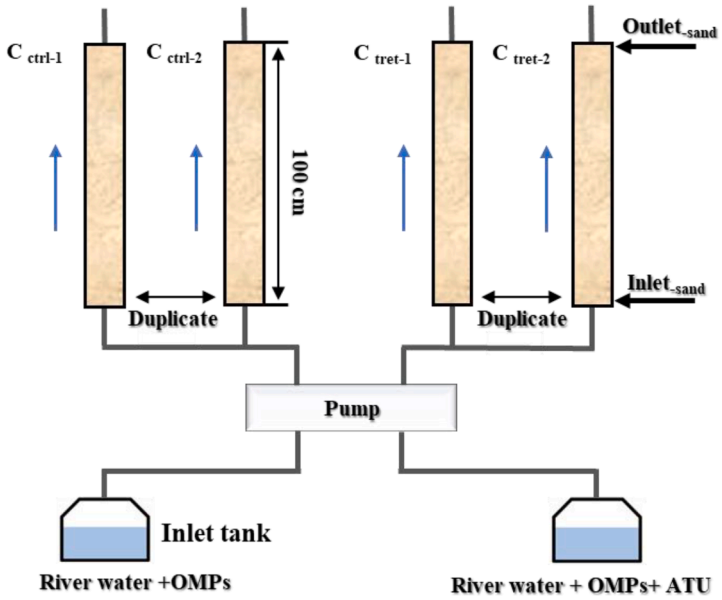

Fig. 1. Experimental set-ups of the column study. OMPs: 128 OMPs with 100 ng/L of each. ATU: 5 mg/L of allylthiourea (ATU) to inhibit AOM.

a 0.45-μm glass fiber filter membrane, to which 0.1 g of Na_2EDTA was added. The pH was then adjusted to approximately 3, and 100 μL of internal standard (28 mixed internal standards of 100 μg/L dissolved in 20% methanol Milli-Q water) was mixed well. The SPE cartridge was activated with 3 mL methanol, 3 mL ultrapure water, and 3 mL ultrapure water (pH = 3). Subsequently, under the negative pressure of the vacuum pump, the water sample was passed through the SPE cartridge at a flow rate of 5–10 mL/min. After filtering the sample, 3 mL of Milli-Q water was added to wash the SPE cartridge, and the water was then drained. The OMPs on the SPE cartridge were eluted by adding 9 mL (3 mL, three times) of methanol. The extract solution was gently blown to dryness under nitrogen (40 °C water bath) and then reconstituted with 0.5 mL solution (80:20 vol/vol Milli-Q water: methanol) before injection.

The 128 OMPs were quantified using a hybrid triple quadrupole ion trap mass spectrometer system (QTRAP 5500 LC-MS/MS, AB SCIEX, USA) equipped with an electrospray ion (ESI) source and coupled to an EXION LC™ AD (AB SCIEX, USA). Liquid chromatography was accomplished using a Phenomenex analytical column (Kinetex 2.6 μm F5 100A, 50 × 3.0 mm) maintained at 40 °C. A 14-min gradient was used, with A:0.1% (vol/vol) high-performance liquid chromatography (HPLC) grade formic acid in Milli-Q water and B: HPLC grade acetonitrile as eluents at 0.4 mL/min flow rate. The liquid phase method was conducted and the mass spectrometry (MS) parameters were set according to the method of Zhao et al. (2022). The mass spectrometry (MS/MS) parameters of the 128 OMPs and 28 internal standards are presented in Tables S1 and S2, respectively. The Multi-Quant software (version 2.0.2) was used for data processing.

2.5. DNA extraction, qPCR assays, and high-throughput sequencing

DNA was extracted from all samples using the Fast DNA® SPIN Kit for Soil (MP Biomedicals, USA), as per the manufacturer's protocol. ATU is reported as an AOM inhibitor (Yan et al., 2022; Srithep et al., 2018; Tran et al., 2014; Vandevivere et al., 1998). The inhibition of AOM activities was confirmed by measuring *amo*A genes with qPCR rather than directly measuring N species (NH_4^+ and NO_2^-/NO_3^-), because of their low concentrations in RBF system. SYBR Green I was used for fluorescence qPCR to evaluate the quantities of AOB, total bacteria, AOA, and total archaea in the sand. The primers used for AOB were AOB *amo*A gene bamoA1F (5′-GGGGTTTCTACTGGTGGT-3′) and bamoA2R (5′-CCCCTCKGSAAAGCCTTCTTC −3′). The primers used for total bacteria were 338F (5′-ACTCCTACGGGAGGCAGCAG-3′) and 806R (5′-GGACTACHVGGGTWTCTAAT-3′), combined with adapter sequences and barcode sequences, respectively. The primers used for AOA were AOA *amo*A gene arch-amoAF (5′-STAATGGTCTGGCTTAGACG-3′) and arch-amoAR (5′-GCGGCCATCCATCTGTATGT −3′). The primers used for the total archaea were arch-524F (5′-TGYCAGCCGCCGCGGTAA-3′) and arch-958R (5′-YCCGGCGTTGAVTCCAATT-3′). The primers used for comammox were *amo*A Nitrospira gene Ntsp-*amo*A 162F (5′-GGATTTCTGGNTSGATTGGA-3′) and Ntsp-*amo*A 359R (5′-WAGTTN-GACCACCASTACCA −3′). The samples were subjected to qPCR using the real-time PCR instrument LineGene9600. The thermal program was 5 min at 95°C, followed by 40 cycles at 95°C for 30 s, 56°C for 30 s (the reaction temperature of the total bacteria was 52°C), and 72°C for 40 s. The amplification system was 20 μL, comprising 2 × ChamQ SYBR Color qPCR Master Mix 10 μL, 0.4 μL each of the forward and reverses primers (5 μM), 2 μL of DNA template, and 7.2 μL of ddH_2O.

The DNA samples were sent to Majorbio Bio-Pharm Technology Co., Ltd. (Shanghai, China) for 16S rRNA gene sequencing. Bacterial DNA was amplified by targeting the V3 to V4 region of the 16S rRNA gene. The universal forward and reverse primers were 515F (5′-GTGCCAGCM GCCGCGGTAA-3′) and 806R (5′-GGACTACVSGGG TATCTAAT-3′), respectively, combined with adapter and barcode sequences. Phusion® High-Fidelity PCR Master Mix (New England Biolabs, Ipswich, MA, USA) was used according to the manufacturer's instructions for PCR. The cycling conditions were 95 °C for 3 min, followed by 27 cycles of 95 °C for 30 s, 55 °C for 30 s, and 72 °C for 45 s, and an elongation step at 72 °C for 10 min. All PCR products were quantified using the Quant-iT™ dsDNA HS Reagent and pooled together. High-throughput sequencing was performed using the HiSeq sequencing platform (Illumina Inc., San Diego, CA, USA). The remaining high-quality paired-end reads (raw sequence reads with filtered low-quality reads and barcode primers) were connected to tags based on overlaps, and the connected tags were analyzed using a standard QIIME pipeline (v1.9.1, http://qiime.org/). The sequences were clustered with operational taxonomic units (OTUs) at a similarity level of 97%. Based on the OTU data, parameters reflecting the abundance and diversity of the microbial community were calculated, including Chao, ACE, Shannon, and Simpson indices, and coverage.

3. Results and discussion

3.1. Water quality and soil microbial community

The DO concentration decreased from 6 mg/L in influents to 2–3 mg/L in effluents during the 82-day OMP exposure experiment (Fig. S1). Meanwhile, the DOC decreased from 6 mg/L in the influent to approximately 4 mg/L in the effluents during the exposure experiment (Fig. S1). The relatively steady DO consumption (50–66%) and DOC removal (33%) implied that stable microbial ecology and bioactivity were established in the columns (Bertelkamp et al., 2014). For both DO and DOC, no significant differences were observed between the control and treatment columns ($C_{ctrl\text{-}1,\ 2}$ vs. $C_{tret\text{-}1,\ 2}$), suggesting the high reliability and reproducibility of the present study. In terms of the soil microbial communities, the Shannon index of inlet$_{sand}$ was significantly lower than that of outlet$_{sand}$ (*t*-test, $p = 0.03$). Among the columns, the Bray–Curtis distance revealed that although the bacterial communities of inlet$_{sand}$ were significantly different, the outlet$_{sand}$ became similar (PCoA, Fig. S2). Within each column, the STAMP analysis demonstrated that the bacterial community composition of inlet$_{sand}$ was clearly different from that of outlet$_{sand}$ (Welch's *t*-test, $p < 0.05$, Fig. S3).

As shown in Table 1, by the end of the column experiment phase 1, the abundance of bacteria decreased significantly from 1.8×10^8 copies/g at inlet$_{sand}$ to 6.2–8.7 $\times 10^6$ copies/g at outlet$_{sand}$ in both the control and treatment columns ($p < 0.001$). In contrast, the abundance of archaea increased from 4.5×10^5 copies/g in inlet$_{sand}$ to 9.2×10^6 copies/g in outlet$_{sand}$ in C $_{ctrl\text{-}1,2}$, which remained stable from inlet$_{sand}$ to outlet$_{sand}$ in C $_{tret\text{-}1,2}$. The relative abundance of archaea increased along with the infiltration distance from 0.5% to 11.7%, indicating that archaea and their associated functions would be non-negligible. Interestingly, independent of the changes in bacteria and archaea, the AOB maintained stable abundances across C $_{ctrl\text{-}1,2}$ and C $_{tret\text{-}1,2}$, AOA increased significantly from inlet$_{sand}$ to outlet$_{sand}$, while the comammox decreased significantly from inlet$_{sand}$ to outlet$_{sand}$ in both groups. In the inlet$_{sand}$, the AOA/AOM (AOA+AOB+ comammox) ratio and comammox/AOM ratio were 23%–72% and 23%–64%, while AOB only counted 5%–13%, suggesting AOA and comammox are dominators of AOM. In the outlet$_{sand}$, AOA counted 94.4%–96.7% and dominated AOM. It is clear that AOM are dominated by AOA and comammox, which can be explained by AOA and comammox being more suitable than AOB for oligotrophic, low-ammonium environments (Leininger et al., 2006; Liu et al., 2011; Straka et al., 2019; Sakoula et al., 2021). In all, the relative abundance of AOM increased from 0.1%–0.2% (inlet$_{sand}$) to 5.3%–5.9% (outlet$_{sand}$).

In phase 2, the abundance of bacteria, archaea and AOA in the inlet$_{sand}$ and outlet$_{sand}$ of each column declined compared with that of phase 1 (Table 1). The decreases of bacteria and archaea might be due to the introduction of the 0.45-μm membrane pre-filtration of feed water in phase 2 that reduced particulate organic matter and prevented the degradation of OMPs before entering the columns (Diem et al., 2013). Additionally, the addition of OMPs might also inhibit bacteria and archaea. Since AOA are autotrophic microbes, whose decreases in $C_{ctrl1,2}$ could be attributed the inhibition effect of OMPs, e.g., antibiotic (Zhao et al., 2022). As for the effect of ATU addition on AOM, AOB and comammox *amo*A genes abundances kept stable in the inlet$_{sand}$ of C $_{ctrl1,2}$ (Table 1), while decreased 22% and 75% in the C $_{tret1,2}$, suggesting the inhibition effect of ATU on them. Notably, AOA *amo*A genes abundances decreased 54% in C $_{ctrl1,2}$, while decreased 86% in C $_{tret1,2}$, more decline occurred in C $_{tret1,2}$ could be attributed to the addition of ATU. The AOM *amo*A genes abundances kept stable in the inlet$_{sand}$ of C $_{ctrl1,2}$, while significantly decreased 78% in the C $_{tret-1,2}$, providing strong evidence that the addition of ATU could inhibit AOM.

Though ATU has been widely recognized and used as AOM inhibitor for investigating the role of AOM in OMPs biotransformation (Yan et al., 2022; Rattier et al., 2014; Srithep et al., 2018; Tran et al., 2014; Vandevivere et al., 1998), some studies found ATU is a non-specific ammonia oxidation inhibitor by comparing with octyne (Men et al., 2017). Octyne can inhibit AOB but not AOA (Taylor et al., 2013), while the degradation of OMPs by AOA strains is non-negligible, e.g., AOA exhibited the best removals of lincomycin, ciprofloxacin, norfloxacin and ofloxacin, followed by comammox and AOB (Zhou et al., 2021). Since AOA were the dominant ammonia oxidizers in the simulated RBF, ATU was chosen as AOM inhibitor in this study. It should be mentioned that ATU is not an exclusive AOM inhibitor (Men et al., 2017). Therefore, though this is currently the best we could achieve, there is a chance that the observed decrease in OMPs removal caused by adding ATU might not be completely resulted from AOM inhibition.

3.2. Efficiency and mechanism of OMP removal

The recoveries of the 128 OMPs ranged from 52% to 145% (Table S5). No significant difference (*t*-test, $p < 0.05$) was found in the performance of duplicate columns (C $_{ctrl\text{-}1}$ vs. C $_{ctrl\text{-}2}$, C $_{tret\text{-}1}$ vs. C $_{tret\text{-}2}$) during the 82-day operation, indicating the high reproducibility and reliability of this study. The data of duplicate columns were merged as a control group (C $_{ctrl\text{-}1,2}$) and a treatment group (C $_{tret\text{-}1,2}$) for the following discussion.

The removal efficiencies of the 128 OMPs over an 82-day experiment are presented in Fig. 2. In general, 31 OMPs were completely removed, and 87 OMPs were partially removed (51 OMPs > 70%, 19 OMPs 30%–70%), suggesting that the simulated first meter of RBF is indeed an effective barrier for most OMPs. Atenolol, caffeine, trimethoprim, and gemfibrozil were removed to a great extent (> 94%), which is similar to the observations in the field RBF sites (Hollender et al., 2018; Regnery et al., 2015; Huntscha et al., 2013). Despite being highly effective for most OMPs, 10 OMPs (such as sulfamethoxazole, carbamazepine, and atenolol acid) broke through the simulated columns and were not removed at all, possibly due to the physicochemical properties of the OMPs (Bertelkamp et al., 2014). As presented in Fig. S4, the OMP removal efficiency was positively correlated with log P and MW but negatively correlated with secondary amides, sulfonamides, ketimines, benzyls, and amines. The secondary sulfonamides were the strongest negatively correlated functional groups; this result complied with previous findings of persistent behaviors of sulfonamides in simulated and

Table 1
qPCR results of total bacteria, total archaea, AOB, AOA, and Comammox. Phase 1: by the end of 6-month microbial cultivation. Phase 2: by the end of the 82-day OMP exposure experiment, feed water of C $_{tret-1,2}$ was added with ATU.

Sampling Information			Abundances of genes (Copies/g)				
Time	Position		Bacterial 16S rRNA	Archaeal 16S rRNA	AOB *amo*A	AOA *amo*A	Comammox *amo*A
Phase 1	C $_{ctrl\text{-}1,2}$	Inlet$_{sand}$	1.8 (±0.2) × 10^8	4.5 (±0.8) × 10^5	1.9 (± 0.3) × 10^4	3.5 (±2.9) × 10^4	9.4 (±2.4) × 10^4
		Outlet$_{sand}$	6.2 (±3.1) × 10^6	9.2 (±5.1) × 10^5	2.0 (±0.7) × 10^4	4.0 (±1.9) × 10^5	3.3 (±1.2) × 10^3
	C $_{tret\text{-}1,2}$	Inlet$_{sand}$	1.8 (±0.2) × 10^8	1.3 (±1.1) × 10^6	1.4 (±0.5) × 10^4	2.0 (±1.8) × 10^5	6.5 (±0.8) × 10^4
		Outlet$_{sand}$	8.7 (±0.2) × 10^6	1.1 (±0.7) × 10^6	1.4 (±0.9) × 10^4	5.0 (±3.2) × 10^5	3.3 (±2.2) × 10^3
Phase 2	C $_{ctrl\text{-}1,2}$	Inlet$_{sand}$	5.9 (±1.6) × 10^7	2.0 (±0.6) × 10^5	1.9 (±0.7) × 10^4	1.6 (±0.9) × 10^4	1.4 (±0.6) × 10^5
		Outlet$_{sand}$	1.3 (±1.2) × 10^6	2.4 (±2.2) × 10^5	5.9 (±0.5) × 10^3	1.4 (±1.2) × 10^5	3.5 (±1.1) × 10^3
	C $_{tret\text{-}1,2}$	Inlet$_{sand}$	1.2 (±0.2) × 10^8	4.0 (±0.6) × 10^5	1.1 (±0.6) × 10^4	2.9 (±1.4) × 10^4	1.6 (±0.6) × 10^4
		Outlet$_{sand}$	1.0 (±0.2) × 10^6	2.7 (±0.5) × 10^5	6.2 (±1.6) × 10^3	1.4 (±0.4) × 10^5	3.0 (±1.5) × 10^3

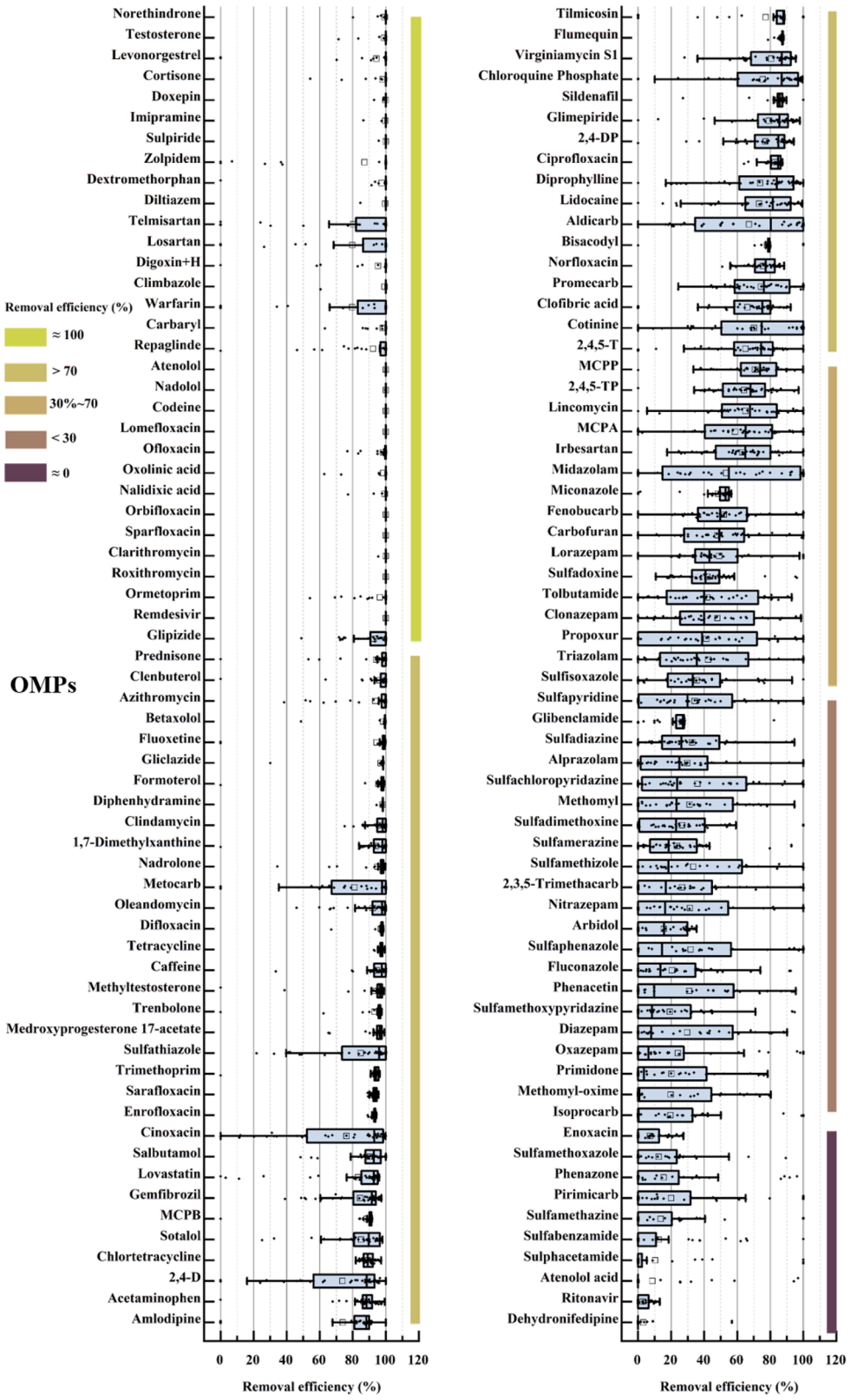

Fig. 2. Removal efficiencies of 128 OMPs (n = 46) in C $_{\text{ctrl-1,2}}$ during the 82-day OMP exposure experiment.

field RBF studies (Bertelkamp et al., 2014; Hamann et al., 2016). This was especially true for sulfamethoxazole, which was not removed in this experiment.

Conflicting results have been obtained from batch tests (only adsorption) and column studies (adsorption and biodegradation) for several OMPs. Specifically, five OMPs with 8%–48% removal in the batch tests were hardly removed in the column study (such as pirimicarb, sulfamethazine, and ritonavir; Fig. S5). This is because the sand adsorbed these OMPs in the short-term batch tests. However, such non-degradable OMPs broke through sand columns and demonstrated

persistent behavior in the long-term study. In contrast, 32 OMPs that were partially or completely removed in the column study (including nadolol and lidocaine) were not removed in the batch test (Fig. S6), suggesting that these OMPs can be removed by biodegradation or biosorption. In other words, these 32 OMPs could only be removed by active microorganisms, thereby emphasizing the key role of microorganisms in the removal of OMPs. Biosorption has been reported to play a negligible role in the removal of OMPs, whereas biodegradation is commonly accepted as the most important mechanism for the removal of OMPs (Bai et al., 2019; Bertelkamp et al., 2014; Huntscha et al., 2013). The correlation between the removal of 32 OMPs and their physicochemical properties demonstrated that MW and log P were positively correlated with the removal efficiencies, whereas secondary amides, secondary sulfonamides, secondary ketimines, benzyls, and primary amines were negatively correlated with the removal efficiencies (Fig. S7). Tertiary amides, secondary ketimines, secondary sulfonamides and tertiary sulfonamides are likely to be most hard-degradable functional groups, followed by secondary amides, benzyl, olefinic bond and phenyl (Fig. S8). Interestingly, with an increase in exposure time, the removal efficiency of 28 OMPs increased (Fig. S9), which might be due

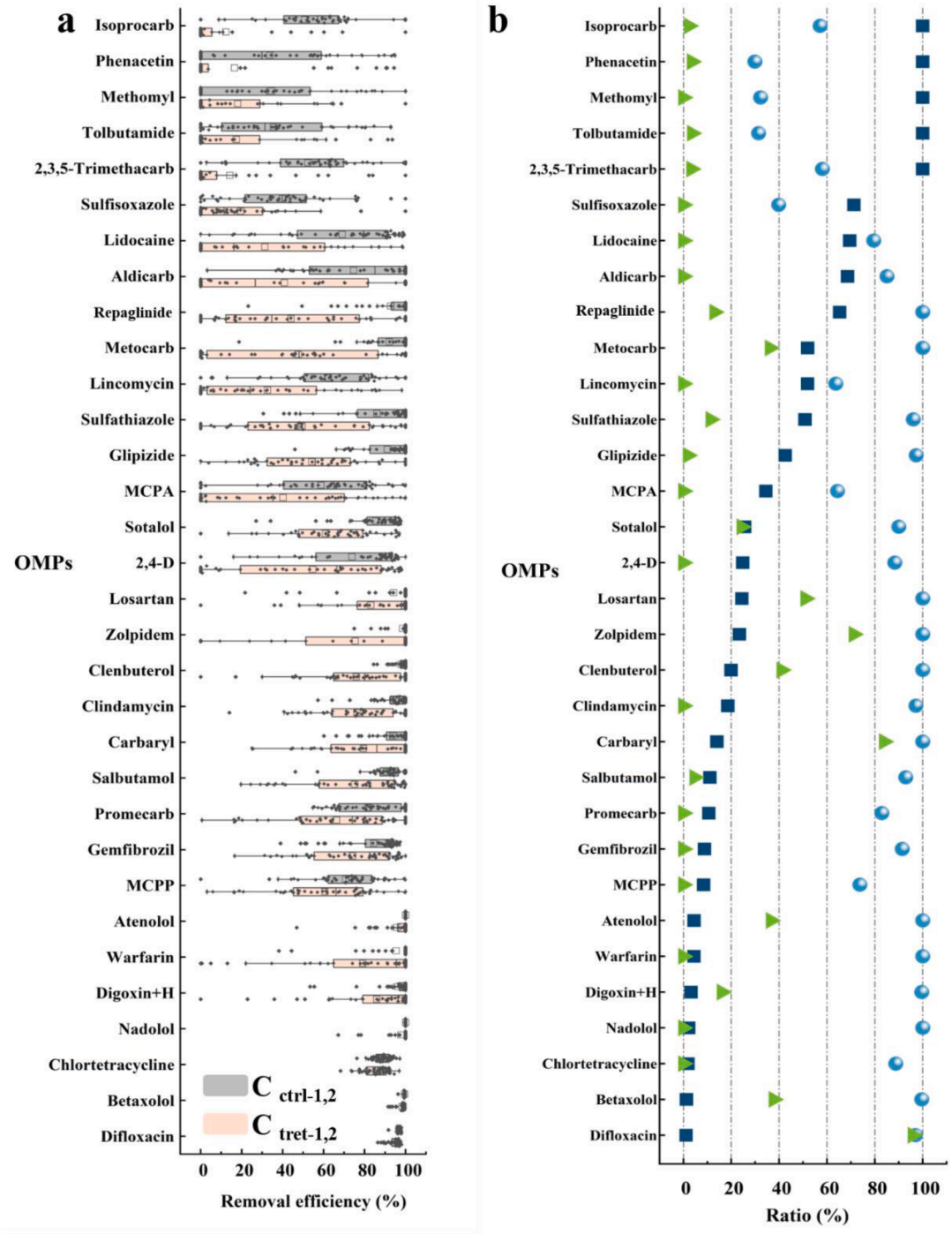

Fig. 3. (a) Thirty-two OMPs with significantly lower removal efficiency in $C_{tret\text{-}1,2}$ than in $C_{ctrl\text{-}1,2}$. (b) The median of removal efficiencies in the column study ($C_{ctrl\text{-}1,2}$). The inhibition ratio of OMP removal efficiency by the addition of ATU. OMP removal efficiency merely through sand adsorption in batch tests.

to genetic changes, enzyme induction, and microbial composition changes (Bertelkamp et al., 2016). In contrast, the removal efficiency of 15 OMPs decreased, indicating the possible occurrence of adsorption saturation, which further implies the refractory biodegradation of these OMPs. Notably, eight identical OMPs (e.g., gemfibrozil, norfloxacin and clofibric acid) were observed in 32 OMPs (only removed by active microorganisms) and 28 OMPs (with increased removal efficiencies), suggesting the sustainability and potential growth of biodegradation in OMPs removal.

3.3. The effects of AOM on OMP removal

The inhibition of AOM significantly decreased the removal efficiency of 32/128 selected OMPs (Fig. 3a). As presented in Fig. 3(b), the degradation of five OMPs, namely, isoprocarb, phenacetin, methomyl, tolbutamide, and 2,3,5-trimethacarb, was nearly completely inhibited; these OMPs were hardly removed by sand adsorption during the batch tests. This suggests a key role of AOM in the removal of certain groups of OMPs in the simulated first meter of RBF. However, the other 13 OMPs (e.g., lidocaine and lincomycin) that could not be removed by sand adsorption were removed by up to 40%–100% by columns via biodegradation. The addition of ATU decreased the removal efficiency by 2%–71%, thereby indicating that these 13 OMPs might be degraded not only by AOM but also by other microorganisms. For example, heterotrophic microorganisms have been reported to degrade EE2, atenolol, and trimethoprim via co-metabolism (Kennes-Veiga et al., 2021; Gusseme et al., 2009; Xu et al., 2017). Moreover, for 14 other OMPs (e.g., repaglinide, atenolol, and difloxacin), it was observed that both sand adsorption (2%–96% removed) and AOM (2–65% inhibited by ATU) contributed to their degradation, while it is unclear whether heterotrophic bacteria play a role in this process. AOM could make negligible or major contribution to the removal of OMP due to the existences of adsorption and heterotrophic microorganisms' degradation, which is depend on the type of OMP.

Among the 32 AOM degradable OMPs in the present study, only the degradation of lincomycin, clindamycin, gemfibrozil, and atenolol transformation by AOM have been documented previously, the mechanism of which were attributed to the reaction of hydroxylation and primary amide hydrolysis induced by the non-specific enzyme of ammonia monooxygenase (AMO) (Fernandez-Fontaina et al., 2012; Rattier et al., 2014; Xu et al., 2017; Helbling et al., 2012; Men et al., 2016; Zhou et al., 2019). Besides, the hydroxylamine, intermediate of ammonia oxidation, could react with lincomycin and achieve $>$ 90% removal (Zhou et al., 2021), and the HNO_2 and NO may also contribute to the biotransformation of OMPs (Yu et al., 2018). It should be noted that the above-mentioned OMPs' degradation via AMO and hydroxylamine were observed in nitrifying activated sludge and AOM pure culture. Since the matrix of organic matter and community of microbes are different, the specific OMPs degradation in the simulated RBF system of the present study might be not exactly the same, which deserves further research.

Moreover, sulfamethoxazole and naproxen, which were classified as non-degradable in the present study, were reported to be degradable by AOM in AOB-dominated high-ammonium eutrophic systems (Kassotaki et al., 2016; Fernandez-Fontaina et al., 2016). It might be reasonable to hypothesis that sulfamethoxazole and naproxen could be degraded by AOB, but not AOA and comammox. Nonetheless, this hypothesis is inconsistent with previous pure culture study which found both AOA and comammox can degradate sulfamethoxazole (Zhou et al., 2019). The contradictory observation in the present study might be attributed to complex bacterial community and different environmental conditions, which may lead to insufficient abundances of AOA and comammox for degrading sulfamethoxazole, or there were microorganisms and/or environmental factors suppressed such function. Differently, it is observed that sotalol was degradable by AOM in the present study, which was not degraded in nitrification enrichment culture (Sathyamoorthy et al., 2013). This might be attributed to the stronger OMP degradation capability of AMO associated with comammox. For example, carbendazim can be degraded by comammox, but not AOA or AOB (Han et al., 2019). In general, the observed variations in OMPs degradation performances of the three ammonia oxidizers could be caused by differences in either microbial community or water quality of the targeted system. Further study in controllable conditions is needed and highly recommended to explore the mechanisms and differences of OMPs transformation by AOA, AOB and comammox.

3.4. Key factors affecting the co-metabolism potential of AOM on OMPs

The inhibition ratio (Y) was defined to assess the contribution of AOM to the degradation of OMPs:

$$Y_x = 100 \times \left(1 - \frac{x's \text{ removal in } C_{tret}}{x's \text{ removal in } C_{ctrl}}\right),$$

where
x – one OMP.
Y_x – the contribution ratio of AOM on the removal of x.

As presented in Fig. 4, the removal efficiencies of OMPs in both the batch tests (RE_{-Batch}) and column studies ($RE_{-Column}$) were negatively correlated with the inhibition ratio, indicating that AOM plays a remarkable role in the degradation of the difficult-to-remove OMPs. The inhibition ratio was also negatively correlated with MW, suggesting that AOM tends to remove OMPs with lower MW. Additionally, the inhibition ratio was positively correlated with log P (32 OMPs, Fig. 4), indicating that OMPs with higher log P values tend to be removed by AOM. Notably, log P was negatively correlated with the removal efficiency of 32 OMPs (Fig. 4) but positively correlated with the removal efficiency of 128 OMPs (Fig. S4). These conflicting observations may be related to the differences in the log P ranges (128 OMPs: −1.5 to 6 vs. 32 OMPs: 0 to 3.5, Fig. S10).

In terms of functional groups, positive correlations were observed between the inhibition ratio and secondary amides, benzyls, secondary sulfonamides, and secondary ketimines (Fig. 4). Secondary amides and benzyls are the two most strongly positively correlated functional groups. The co-metabolism of OMPs containing amides by AOM has been reported in wastewater treatment plants, where atenolol is biotransformed to atenolol acid through primary amide hydrolysis by AOB (Helbling et al., 2012; Xu et al., 2017), and lincomycin with secondary amide is biodegraded by AOM (Zhou et al., 2021). It is reasonable to hypothesize that hydrolysis of primary and/or secondary amides by AOM might occur for the 16 OMPs containing amides (e.g., atenolol, lincomycin, and isoprocarb). In addition, 4/8 of the benzyl-containing OMPs did not contain nitrogen functional groups (i.e., secondary amides and secondary sulfonamides), implying that the strong positive correlation between benzyls and the inhibition ratio may be attributed to ammonia monooxygenase-mediated C—H hydroxylation of aliphatic compounds (Su et al., 2021). Interestingly, among the 13/128 OMPs containing tertiary amide groups, only the degradation of zolpidem, which contains both tertiary amides and benzyls, was inhibited. Hence, the inhibition of zolpidem degradation was due to benzyls rather than tertiary amides, suggesting that the co-metabolism of AOM could not act on tertiary amides. The observed positive correlation between the inhibition ratio and secondary sulfonamides complied with previous findings of the degradation of sulfadiazine and sulfamethoxazole (containing secondary sulfonamides) by AOB in wastewater treatment processes (Wang et al., 2019; Kassotaki et al., 2016). Meanwhile, the removal of sildenafil-containing tertiary sulfonamides (not containing secondary amides, benzyls, and secondary sulfonamides) was not inhibited, suggesting that tertiary sulfonamides may not be transformed by AOM. Overall, the ability of certain OMPs to be co-metabolically

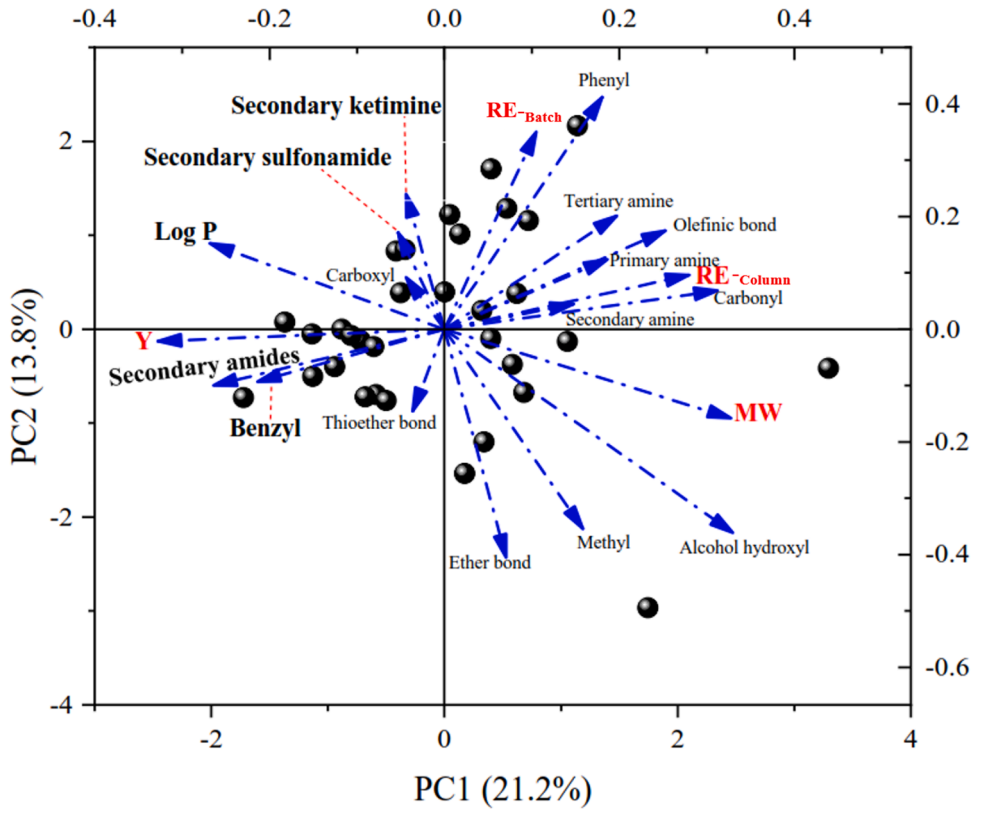

Fig. 4. Correlation analysis graph between the participation of AOM in the removal of 32 OMPs and the physical and chemical properties of OMPs (MW, log P, and the number of nitrogen-containing functional groups). Y: removal efficiency inhibition ratio, the degree of participation of AOM in the degradation of OMPs; $RE\text{-}_{Column}$: removal efficiency through biodegradation and adsorption; $RE\text{-}_{Batch}$: removal efficiency only by adsorption; MW: molecular weight.

degraded by AOM is largely determined by their physicochemical properties. More specifically, OMPs with lower MW containing primary amide, benzyl, secondary amide, and secondary sulfonamide groups are more likely to be degraded by AOM.

3.5. Environmental relevance and implications

Recently, there has been an increasing concern regarding the presence and potential risk of OMPs in urban water system, especially in drinking water (Hollender et al., 2018; Kondor et al., 2020; Li et al., 2021). It is an urgent need to develop green and effective barrier that can remove target OMPs, while avoid generation of byproducts with low additional cost. This study focuses on nature-based RBF system and its OMPs biodegradation mechanism. Though it has been widely observed that RBF performed well regarding OMPs removal through biodegradation, such bio-process remains poorly documented, which hampered the application and improvements of OMPs removal in drinking water systems (Bertelkamp et al., 2014; Hamann et al., 2016; Kondor et al., 2020).

This work determined the removal efficiencies of 128 OMPs in the simulated first-meter of RBF, of which 82 OMPs were > 70%, highlighting the important role of the oxic zone. Combined the results from the column and batch experiments, it can be concluded that the removals of 32 OMPs were entirely accomplished via biodegradation, suggesting a critical contribution of biodegradation on OMPs' removal in RBF. For those OMPs, the observed correlations between OMPs' functional groups and their corresponding biodegradation potential are valuable for predicting the fate of OMPs in RBF. Interestingly, the removal efficiency of 28 OMPs increased with exposure time, indicating there might be adaption time needed for biofiltration to remove OMPs.

The role of AOM in OMPs' biodegradation was studied by ATU inhibition experiments, which showed the OMPs biodegradation is achieved by both AOM and non-AOM microbes. Considering the functional groups, AOM tend to degrade OMPs containing primary amide, benzyl, secondary amide, and secondary sulfonamide. The finding sheds new light on the correlation between physiochemical properties of OMPs and their AOM co-metabolic potential, based on which prediction could be made when new OMPs present in source water. On this basis, the OMPs removal could be enhanced, and necessary subsequent treatments can be adjusted to minimize the risk of new OMPs. The mechanism of OMPs transformation by AOM might be different among water systems such as WWTPs, wetlands and RBF. However, the obtained knowledge about the functional groups of OMPs and their AOM co-metabolic potential may be helpful for understanding the OMPs degradation in other water systems. It should be noted that the activities of AOA, AOB and comammox were simultaneously inhibited by ATU in this study, which might also inhibit other enzymes. To explore the specific contribution of each AOM precisely, strategies should be developed for inhibiting the microbes separately and exclusively.

4. Conclusions

Based on the simulated first-meter infiltration of RBF in this study, it can be concluded that

- Most of the OMPs were effectively removed. Among the 128 OMPs, the removal efficiencies of 82 OMPs were above 70% (31 OMPs were completely removed), 15 OMPs were 30%–70%, and 31 OMPs were below 30% (10 OMPs were not removed at all).
- Biodegradation was the most important factor followed by adsorption. Inefficiently removed OMPs tended to have low MW, low log P, and contain secondary amide, sulfonamide, ketimine, and benzyl groups.

- The relative abundance of AOM increased with infiltration distance from 0.2% to 5.9%, in which AOA accounted for 23%–72% (inlet$_{-sand}$) to 97% (outlet$_{-sand}$), comammox accounted for 1% (outlet$_{-sand}$) to 23%–64% (inlet$_{-sand}$). The abundances of AOM *amo*A genes decreased 78%, suggesting the inhibition effects of ATU on AOM.
- AOM play an important role in this process. Inhibiting AOM suppressed the degradation of 32 OMPs, five of which were almost completely inhibited.
- OMPs with low MW and containing primary amide, secondary amide, secondary sulfonamide, and benzyl groups are more likely to be removed by AOM.

Declaration of Competing Interest

The authors declare that they have no known competing financial interests or personal relationships that could have appeared to influence the results presented in this paper.

Data Availability

Data will be made available on request.

Acknowledgments

This work was supported by the National Natural Science Foundation of China (Grant No. 51820105011, 52091542).

Supplementary materials

Supplementary material associated with this article can be found, in the online version, at doi:10.1016/j.watres.2022.119250.

References

Bai, Y., Ruan, X., Wang, F., Antoine, G., Hoek, J., 2019. Sulfonamides removal under different redox conditions and microbial response to sulfonamides stress during riverbank filtration: a laboratory column study. Chemosphere 220, 668–677.
Bertelkamp, C., Reungoat, J., Cornelissen, E.R., Singha, N., Reynisson, J., Cabo, A.J., Hoek, J., Verliefde, A., 2014. Sorption and biodegradation of organic micropollutants during river bank filtration: a laboratory column study. Water Res. 52, 231–241.
Bertelkamp, C., Verliefde, A., Schoutteten, K., Vanhaecke, L., Bussche, J.V., Singhal, N., Hoek, J., 2016. The effect of redox conditions and adaptation time on organic micropollutant removal during river bank filtration: a laboratory-scale column study. Sci. Total Environ. 544, 309–318.
Borrull, J., Colom, A., Fabregas, J., Borrull, F., Pocurull, E., 2021. Presence, behaviour and removal of selected organic micropollutants through drinking water treatment. Chemosphere 276, 130023.
Bu, Q., Wang, B., Huang, J., Deng, S., Yu, G., 2013. Pharmaceuticals and personal care products in the aquatic environment in China: a review. J. Hazard. Mater. 262, 189–211.
Covatti, G., Grischek, T., 2021. Sources and behavior of ammonium during riverbank filtration. Water Res. 191, 116788.
Diem, S., Rudolf Von Rohr, M., Hering, J.G., Kohler, H.E., Schirmer, M., von Gunten, U., 2013. NOM degradation during river infiltration: effects of the climate variables temperature and discharge. Water Res. 47, 6585–6595.
Fernandez-Fontaina, E., Gomes, I.B., Aga, D.S., Omil, F., Lema, J.M., Carballa, M., 2016. Biotransformation of pharmaceuticals under nitrification, nitratation and heterotrophic conditions. Sci. Total Environ. 541, 1439–1447.
Fernandez-Fontaina, E., Omil, F., Lema, J.M., Carballa, M., 2012. Influence of nitrifying conditions on the biodegradation and sorption of emerging micropollutants. Water Res. 46, 5434–5444.
Fowler, S.J., Palomo, A., Dechesne, A., Mines, P.D., Smets, B.F., 2018. Comammox Nitrospira are abundant ammonia oxidizers in diverse groundwater-fed rapid sand filter communities. Environ. Microbiol. 20, 1002–1015.
Gusseme, B.D., Pycke, B., Hennebel, T., Marcoen, A., Vlaeminck, S.E., Noppe, H., Boon, N., Verstraete, W., 2009. Biological removal of 17α-ethinylestradiol by a nitrifier enrichment culture in a membrane bioreactor. Water Res. 43, 2493–2503.
Hamann, E., Stuyfzand, P.J., Greskowiak, J., Timmer, H., Massmann, G., 2016. The fate of organic micropollutants during long-term/long-distance river bank filtration. Sci. Total Environ. 545-546, 629–640.
Han, P., Yu, Y., Zhou, L., Tian, Z., Li, Z., Hou, L., Liu, M., Wu, Q., Wagner, M., Men, Y., 2019. Specific micropollutant biotransformation pattern by the comammox bacterium nitrospira inopinata. Environ. Sci. Technol. 53, 8695–8705.
Helbling, D.E., Johnson, D.R., Honti, M., Fenner, K., 2012. Micropollutant biotransformation kinetics associate with WWTP process parameters and microbial community characteristics. Environ. Sci. Technol. 46, 10579–10588.
Hollender, J., Rothardt, J., Radny, D., Loos, M., Epting, J., Huggenberger, P., Borer, P., Singer, H., 2018. Comprehensive micropollutant screening using LC-HRMS/MS at three riverbank filtration sites to assess natural attenuation and potential implications for human health. Water Res. X 1, 100007.
Huntscha, S., Rodriguez Velosa, D.M., Schroth, M.H., Hollender, J., 2013. Degradation of polar organic micropollutants during riverbank filtration: complementary results from spatiotemporal sampling and push–pull tests. Environ. Sci. Technol. 47, 11512–11521.
Junier, P., Molina, V., Dorador, C., Hadas, O., Kim, O., Junier, T., Witzel, K., Imhoff, J.F., 2010. Phylogenetic and functional marker genes to study ammonia-oxidizing microorganisms (AOM) in the environment. Appl. Microbiol. Biotechnol. 85, 425–440.
Kassotaki, E., Buttiglieri, G., Ferrando-Climent, L., Rodriguez-Roda, I., Pijuan, M., 2016. Enhanced sulfamethoxazole degradation through ammonia oxidizing bacteria co-metabolism and fate of transformation products. Water Res. 94, 111–119.
Kennes-Veiga, D.M., Gonzalez-Gil, L., Carballa, M., Lema, J.M., 2021. The organic loading rate affects organic micropollutants' cometabolic biotransformation kinetics under heterotrophic conditions in activated sludge. Water Res. 189, 116587.
Kits, K.D., Sedlacek, C.J., Lebedeva, E.V., Han, P., Bulaev, A., Pjevac, P., Daebeler, A., Romano, S., Albertsen, M., Stein, L.Y., Daims, H., Wagner, M., 2017. Kinetic analysis of a complete nitrifier reveals an oligotrophic lifestyle. Nature 549, 269–272.
Kondor, A.C., Jakab, G., Vancsik, A., Filep, T., Szeberényi, J., Szabó, L., Maász, G., Ferincz, Á., Dobosy, P., Szalai, Z., 2020. Occurrence of pharmaceuticals in the Danube and drinking water wells: efficiency of riverbank filtration. Environ. Pollut. 265, 114893.
Leininger, S., Urich, T., Schloter, M., Schwark, L., Qi, J., Nicol, G., Prosser, J., Schuster, S., Schleper, C., 2006. Archaea predominate among ammonia-oxidizing prokaryotes in soils. Nature 442, 806–809.
Li, X., Zhang, R., Tian, T., Shang, X., Du, X., He, Y., Matsuura, N., Luo, T., Wang, Y., Chen, J., Kadokami, K., 2021. Screening and ecological risk of 1200 organic micropollutants in Yangtze Estuary water. Water Res. 201, 117341.
Limpiyakorn, T., Sonthiphand, P., Rongsayamanont, C., Polprasert, C., 2011. Abundance of amoA genes of ammonia-oxidizing archaea and bacteria in activated sludge of full-scale wastewater treatment plants. Bioresour. Technol. 102, 3694–3701.
Liu, Z., Huang, S., Sun, G., Xu, Z., Xu, M., 2011. Diversity and abundance of ammonia-oxidizing archaea in the Dongjiang River. China. Microbiol. Res. 166, 337–345.
Loos, R., Carvalho, R., António, D.C., Comero, S., Locoro, G., Tavazzi, S., Paracchini, B., Ghiani, M., Lettieri, T., Blaha, L., Jarosova, B., Voorspoels, S., Servaes, K., Haglund, P., Fick, J., Lindberg, R.H., Schwesig, D., Gawlik, B.M., 2013. EU-wide monitoring survey on emerging polar organic contaminants in wastewater treatment plant effluents. Water Res. 47, 6475–6487.
Men, Y., Achermann, S., Helbling, D.E., Johnson, D.R., Fenner, K., 2017. Relative contribution of ammonia oxidizing bacteria and other members of nitrifying activated sludge communities to micropollutant biotransformation. Water Res. 109, 217–226.
Men, Y., Han, P., Helbling, D.E., Jehmlich, N., Herbold, C., Gulde, R., Onnis-Hayden, A., Gu, A.Z., Johnson, D.R., Wagner, M., Fenner, K., 2016. Biotransformation of two pharmaceuticals by the ammonia-oxidizing archaeon nitrososphaera gargensis. Environ. Sci. Technol. 50, 4682–4692.
Miyawaki, T., Nishino, T., Asakawa, D., Haga, Y., Hasegawa, H., Kadokami, K., 2021. Development of a rapid and comprehensive method for identifying organic micropollutants with high ecological risk to the aquatic environment. Chemosphere 263, 128258.
Oberleitner, D., Schulz, W., Bergmann, A., Achten, C., 2020. Impact of seasonality, redox conditions, travel distances and initial concentrations on micropollutant removal during riverbank filtration at four sites. Chemosphere 250, 126255.
Rattier, M., Reungoat, J., Keller, J., Gernjak, W., 2014. Removal of micropollutants during tertiary wastewater treatment by biofiltration: role of nitrifiers and removal mechanisms. Water Res. 54, 89–99.
Regnery, J., Barringer, J., Wing, A.D., Hoppe-Jones, C., Teerlink, J., Drewes, J.E., 2015. Start-up performance of a full-scale riverbank filtration site regarding removal of DOC, nutrients, and trace organic chemicals. Chemosphere 127, 136–142.
Robles-Molina, J., Lara-Ortega, F.J., Gilbert-López, B., García-Reyes, J.F., Molina-Díaz, A., 2014. Multi-residue method for the determination of over 400 priority and emerging pollutants in water and wastewater by solid-phase extraction and liquid chromatography-time-of-flight mass spectrometry. J. Chromatogr. A 1350, 30–43.
Sakoula, D., Koch, H., Frank, J., Jetten, M.S.M., van Kessel, M.A.H.J., Lücker, S., 2021. Enrichment and physiological characterization of a novel comammox Nitrospira indicates ammonium inhibition of complete nitrification. ISME J. 15, 1010–1024.
Sathyamoorthy, S., Chandran, K., Ramsburg, C.A., 2013. Biodegradation and cometabolic modeling of selected beta blockers during ammonia oxidation. Environ. Sci. Technol. 47, 12835–12843.
Srithep, P., Pornkulwat, P., Limpiyakorn, T., 2018. Contribution of ammonia-oxidizing archaea and ammonia-oxidizing bacteria to ammonia oxidation in two nitrifying reactors. Environ. Sci. Pollut. Res. 25, 8676–8687.
Stein, L.Y., 2019. Insights into the physiology of ammonia-oxidizing microorganisms. Curr. Opin. Chem. Biol. 49, 9–15.
Straka, L.L., Meinhardt, K.A., Bollmann, A., Stahl, D.A., Winkler, M.H., 2019. Affinity informs environmental cooperation between ammonia-oxidizing archaea (AOA) and anaerobic ammonia-oxidizing (Anammox) bacteria. ISME J. 13, 1997–2004.
Su, Q., Schittich, A., Jensen, M.M., Ng, H., Smets, B.F., 2021. Role of ammonia oxidation in organic micropollutant transformation during wastewater treatment: insights

from molecular, cellular, and community level observations. Environ. Sci. Technol. 55, 2173–2188.
Taylor, A.E., Vajrala, N., Giguere, A.T., Gitelman, A.I., Arp, D.J., Myrold, D.D., Sayavedra-Soto, L., Bottomley, P.J., 2013. Use of aliphatic *n*-alkynes to discriminate soil nitrification activities of ammonia-oxidizing thaumarchaea and bacteria. Appl. Environ. Microbiol. 79, 6544–6551.
Tran, N.H., Nguyen, V.T., Urase, T., Ngo, H.H., 2014. Role of nitrification in the biodegradation of selected artificial sweetening agents in biological wastewater treatment process. Bioresour. Technol. 161, 40–46.
Vandevivere, P., Ficara, E., Terras, C., Julies, E., Verstraete, W., 1998. Copper-mediated selective removal of nitrification inhibitors from industrial wastewaters. Environ. Sci. Technol. 32, 1000–1006.
Wang, Y., Ma, L., Mao, Y., Jiang, X., Xia, Y., Yu, K., Li, B., Zhang, T., 2017. Comammox in drinking water systems. Water Res. 116, 332–341.
Wang, B., Ni, B.J., Yuan, Z., Guo, J., 2019. Cometabolic biodegradation of cephalexin by enriched nitrifying sludge: process characteristics, gene expression and product biotoxicity. Sci. Total Environ. 672, 275–282.
Xu, Y., Radjenovic, J., Yuan, Z., Ni, B.J., 2017. Biodegradation of atenolol by an enriched nitrifying sludge: products and pathways. Chem. Eng. J. 312, 351–359.
Yan, R., Wang, Y., Li, J., Wang, X., Wang, Y., 2022. Determination of the lower limits of antibiotic biodegradation and the fate of antibiotic resistant genes in activated sludge: both nitrifying bacteria and heterotrophic bacteria matter. J. Hazard. Mater. 425, 127764.
Yu, Y., Han, P., Zhou, L., Li, Z., Wagner, M., Men, Y., 2018. Ammonia monooxygenase-mediated cometabolic biotransformation and hydroxylamine-mediated abiotic transformation of micropollutants in an AOB/NOB coculture. Environ. Sci. Technol. 52, 9196–9205.
Zhang, Y., Duan, L., Wang, B., Liu, C.S., Jia, Y., Zhai, N., Blaney, L., Yu, G., 2020. Efficient multiresidue determination method for 168 pharmaceuticals and metabolites: optimization and application to raw wastewater, wastewater effluent, and surface water in Beijing, China. Environ. Pollut. 261, 114113.
Zhou, L., Han, P., Zhao, M., Yu, Y., Sun, D., Hou, L., Liu, M., Zhao, Q., Tang, X., Klümper, U., Gu, J., Men, Y., Wu, Q.L., 2021. Biotransformation of lincomycin and fluoroquinolone antibiotics by the ammonia oxidizers AOA, AOB and comammox: a comparison of removal, pathways, and mechanisms. Water Res. 196, 117003.
Zhou, L., Han, P., Yu, Y., Wang, B., Men, Y., Wagner, M., Wu, Q.L., 2019. Cometabolic biotransformation and microbial-mediated abiotic transformation of sulfonamides by three ammonia oxidizers. Water Res. 159, 444–453.
Zuo, R., Pan, M., Li, J., Meng, L., Yang, J., Zhai, Y., Xue, Z., Liu, J., Shi, J., Teng, Y., 2021. Biogeochemical transformation processes of iron, manganese, ammonium under coexisting conditions in groundwater based on experimental data. J. Hydrol. 603, 127120.
Zhao, J., Fang, S., Qi, W., Liu, H., Qu, J., 2022a. Do NH_4^+-N and AOB affect atenolol removal during simulated riverbank filtration? Chemosphere 301, 134653.
Zhao, J., Fan, X., Li, X., Gao, Y., Zhang, Z., 2022b. Impact of ciprofloxacin and copper combined pollution on activated sludge: abundant-rare taxa and antibiotic resistance genes. Bioresource Technol 349, 126882.
Zhai, Y., Liu, G., van der Meer, W.G.J., 2022. One-step reverse osmosis based on riverbank filtration for future drinking water purification. Engineering 9, 27–34.